Influence of solvents on the morphology of Langmuir and Langmuir–Schaefer films of PCBM and PCBM-based oligomers and polymers

Lucas K M Roncaselli, Edilene A Silva, Maria Luisa Braunger, Hasina H. Ramanitra, Meera Stephen, Lucas V L Citolino, José D Fernandes, André Simõis, Carlos J L Constantino, Deuber Lincon Silva Agostini, et al.

Influence of the solvents in the morphology of Langmuir and Langmuir-Schaefer films of PCBM and PCBM-based oligomers and polymers

Lucas K. M. Roncaselli[a], Edilene A. Silva[b], Maria Luisa Braunger[a], Hasina H. Ramanitra[c], Meera Stephen[c], Lucas V. L. Citolino[a], José D. Fernandes[a], André V. S. Simõis[a], Carlos J. L. Constantino[a], Deuber Lincon Silva Agostini[a], Didier Bégué[c], Roger C. Hiorns[c]*, Clarissa A. Olivati[c]*

Fullerene-based polymers and oligomers combined with non-fullerene acceptors are showing extremely high efficiencies in organic photovoltaic devices. Furthermore, fullerene-based materials are of interest for use in anti-cancer and anti-viral treatments, where their presence can enhance the efficacity of the medication considerably. Therefore, it remains important to understand their morphology and electronic properties to improve devices and technological applications. The main goal of this study is to prepare and characterize Langmuir and Langmuir-Schaefer films of PCBM-based materials to investigate the influence of different solvents such as chloroform, toluene, and xylene, and co-components on their morphology. The PCBM-based materials were thus studied either alone or in mixtures with a polythiophene derivative (poly(3-hexythiophene), P3HT) commonly used in organic photovoltaic devices. The formation of Langmuir films was studied using surface pressure isotherms and Brewster's angle microscopy (BAM), where information on the homogeneity, phase behavior, and morphology of the films were analyzed. In addition, Langmuir-Schaefer films were characterized by UV-visible absorption spectroscopy, atomic force microscopy (AFM), and Raman spectroscopy, providing information on the morphology of the solid films. This study has shown it is possible to successfully fabricate Langmuir and Langmuir-Schaefer films of PCBM and PCBM-based oligomers and polymers, both pure and mixed with P3HT, to compare their organization, roughness, and optical properties. With the Langmuir films, it was possible to estimate the area of the molecules and visualize their aggregation through BAM images, establishing a relationship between the area occupied by these materials and the solvent used. All characterization techniques corroborate that the use of chloroform significantly reduced the roughness of LS films mixed with P3HT and also presented a higher ordering compared to films prepared with xylene solutions.

Introduction

It remains important to understand the aggregative and electronic properties of fullerenes, their derivatives and their polymers. While they have been overtaken by the prodigious rise in non-fullerene acceptors (NFAs) in organic photovoltaic devices (OPVs),[1,2,3] those devices that combine both NFAs and fullerenes are showing extremely high efficiencies.[4] Furthermore, fullerenes are of interest for use in anti-cancer[5,6] and anti-viral treatments,[7] where their presence is able to enhance the efficacity of the medication. The interest in fullerenes stems from their exceptional electron affinity and, to some extent, their complementary absorption at low wavelengths. However, in all these applications, and especially in biological and medical fields, the exploitation of the properties of fullerenes has been greatly hampered by limited knowledge of how to control their aggregative behavior. They tend to form dimers and aggregates in an uncontrolled manner,[8,9] and this coupled with their highly hydrophobic nature, further limits their photovoltaic and biological exploitation. An understanding of the aggregative behaviors of fullerenes, and their derivatives would allow a better understanding of the formation of their aggregates and consequently how to go about improving their behavior, how to incorporate them into other structures, for example, block copolymers, and how to better exploit their properties.

While the higher fullerenes, such as those based on C_{70} are used in high-end applications, due to cost and ease of access C_{60}-based materials remain *de-facto* materials for study. The most widely used fullerene derivative is [6,6]-phenyl C_{61} butyric acid methyl ester (PCBM) with the modified sphere permitting good solubility in common organic solvents.[10,11,12] The chemical modification of fullerene is based on radical,[13] cyclo-additions,[14] and nucleophilic additions.[15] This chemistry has given birth to the aforementioned PCBM but also to a range of oligomeric and polymeric structures.[12] The incorporation of fullerene or PCBM into the main-chain of an oligomer or polymer is of considerable interest because there is atomic economy – they make up part of the skeletal structure – and they tend to show less aggregation than polymers which have fullerenes as functional pendent groups.[16] Furthermore, by way of making two additions to the sphere, it is possible to have considerable control over the electronic properties of fullerene.

In this work, our study was limited to PCBM, a main-chain PCBM oligomer and a main-chain PCBM polymer.

The techniques used to manufacture thin-films are also fundamental, among them Langmuir-based techniques which are ideal for the study of these (macro)molecules because they can be used to closely follow their aggregative behaviors.[17,18] Due to the hydrophobic characteristics of PCBM and poly(fullerene)s, it is possible to characterize the organization of these materials as monolayers under well-defined experimental conditions. While the technique was originally applied to long-chain fatty acids and alcohols,[19] more recent developments, careful control of the solvation of the products, film formation, and film collection have made it possible to consider more complex, hydrophobic (macro)molecules such polymeric electron donors and acceptors.[20] Langmuir films can be transferred to a solid substrate by Langmuir-Blodgett (LB) or Langmuir-Schaefer (LS) techniques, which have the main advantage of preparing films with oriented molecular structures, at least for amphiphilic molecules.[21] With more oriented structures it is possible to improve some features of the solid films and therefore to achieve higher devices efficiencies in organic electronic applications.[22]

Here, we study the properties of three fullerene-based materials, namely PCBM, a main-chain PCBM oligomer and a main-chain PCBM polymer, and consider their intrinsic behavior with

respect to their self-assembly and aggregation. For this purpose, the behavior of these materials solubilized in different organic solvents was evaluated in a Langmuir trough. The materials were deposited onto solid substrates using the Langmuir-Schaefer technique to evaluate the influence of the organic solvent on the solid film features that are of direct relevance to devices manufacture. Moreover, the investigation of different properties of fullerenes together with P3HT was carried out due to its high potential for application in organic electronic devices. In this work, we were able to evaluate the impact of size and nature of the pure fullerene-based materials, and with P3HT, on their aggregative behavior, to gain a better understanding of the morphology of the film's structure-aggregation relationships.

Materials and Methods

Materials

Syntheses of oligomers and polymers were performed in flame-dried, dry-nitrogen flushed glass reactors using solvents that had been distilled from over their respective drying agents under dry nitrogen. Otherwise, materials were used as received and obtained from Aldrich (France), except for P3HT which came from Aldrich (Brazil) and PCBM from Merck KGaA (Germany). UV light was filtered from laboratory windows and fluorescent lights.

^{1}H (400.6 MHz), ^{13}C (100.16 MHz), and 2-D NMRs were recorded on a Bruker® Avance 400 spectrometer at ambient temperature using solvents as indicated. Characterisations using size exclusion chromatography (SEC) were performed either: at 30 °C with THF as eluent at a flow rate of 1 mL min^{-1}, a toluene flow marker, a bank of 4 columns (Shodex KF801, 802.5, 804, and 806) each of length 300 mm and diameter 8, the whole controlled by Malvern pump (Viskotek, VE1122) connected to Malvern VE3580 refractive index and VE3210 UV-visible detectors; or at 50 ˚C with HPLC grade chlorobenzene as eluent at a flow rate of 1 mL min^{-1} through a PLgel 10 µm Mixed-B (300 × 7.5 mm) SEC column controlled by an Agilent Technologies 1260 system and characterised with a refractive index detector. Calibration was against polystyrene standards and samples (0.5 to 4 mg mL^{-1}) were pre-filtered.

The oligomer, oligo{(phenyl-C_{61}-butyric acid methyl ester)-*alt*-[1,4-bis(bromomethyl)-2,5-bis(octyloxy)benzene]} (OPCBMMB) and the polymer poly{[bispyrrolidino(phenyl-C_{61}-butyric acid methyl ester)]-*alt*-[2,5-bis(octyloxy)benzene]} (PPCBMB), both based on PCBM, were prepared and characterized as previously described.[23,24] PCBM and the repeating units of OPCBMMB and PPCBMB have molar masses of 910.9 g mol^{-1}, 1295.4 g mol^{-1} and 1383.5 g mol^{-1}, respectively.

The PCBM-based materials were studied either alone in solution or in mixtures with poly(3-hexylthiophene) (P3HT), which has a repeating unit molar mass of 166 g.mol^{-1}. Figure 1 shows the chemical structures of the materials used in this study.

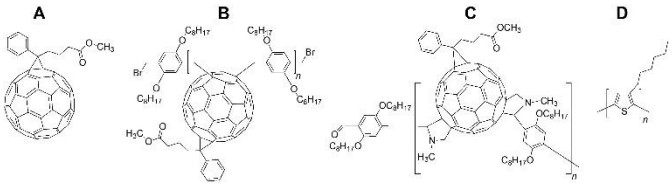

Figure 1. Materials used, from left to right: a) PCBM; b) OPCBMMB; c) PPCBMB; and d) P3HT.

Synthesis of fullerene derivatives

With regards to the synthetic method used to prepare the fullerene-based oligomer and polymer, it is important to highlight that there are six known methods to incorporate fullerenes into a polymer main chain.[25,26,27,28,23,29,30] In all these methods, a comonomer is required to undergo the addition chemistry to form the bridge between each fullerene. In our work, we chose to study products resulting from the so-called atom transfer radical addition polymerization (ATRAP),[31] which generally gives rise to short oligomers, and by the sterically controlled azomethine ylide cycloaddition polymerization (SACAP) which yields relatively high molecular weight polymers.[24] While the ATRAP system shows weak bonds between C_{60}s, due to single methylene links,[32] the SACAP-based polymers are extremely robust due to the cyclic-nature of the additions to the spheres.[33,34]

OPCBMMB is the same sample as that prepared in reference 35 by the ATRAP route. For the sake of completeness, its preparation is described here. PCBM (3 g, 3.28 x 10^{-3} mol) and 1,4-bis(bromomethyl)-2,5-bis(octyloxy)benzene (1.71 g, 3.28 x 10^{-3} mol) were stirred in toluene (150 mL). CuBr (0.158 g, 1 x 10^{-3} mol) and bipyridine (2.06 g, 13.2 x 10^{-3} mol) were added and the temperature was raised to 100 °C. After 16 h, and recovery by precipitation in methanol (500 mL), the product was Soxhlet-washed with acetone for three days. Drying under reduced pressure yielded a dark brown powder (2.07 g, 49%). Deconvolution of the UV-visible GPC indicated that PCBM made up 35% by mass of the sample. ^{1}H NMR (400 MHz, C_6D_6) δ = 0.9 (s, -OC_7H_{14}-CH_3), 1.20-1.71 (m, broad, O-CH_2-C_6H_{12}-CH_3), 1.95-2.38 (m,-C_3H_6-C=OOCH_3), 2.75 (s, O-CH_2-C_6H_{12}-CH_3), 3.33 (s, -O-CH_3), 3.65-3.87 (broad, O-CH_2-C_6H_{12}-CH_3), 3.88-4.30 (broad, C_{60}-CH_2-ph), 4.31-4.65 (broad, -CH_2-Br), 7.22-7.68 (m, *aromatic*) ppm; ^{13}C NMR (101 MHz, C_6D_6) δ = 14.1 (-OC_7H_{14}-CH_3), 22.3-33.0 (O-CH_2-C_6H_{12}-CH_3, CH_2-Br), 50.8-51.9 (-O-CH_3), 69.5 (O-CH_2-C_6H_{12}-CH_3), 114.7-117.8 (*aromatic*), 132.0 (*aromatic*-PCBM), 136.8-148.8 (*fullerene cage*), 172.3 (C=O) ppm.

PPCBMB was prepared by the SACAP route as detailed in reference 24. Again, the preparative route is detailed here for the sake of completeness. 2,5-Bis(octyloxy)terephthalaldehyde (0.21 g, 0.55 mmol), $PC_{60}BM$ (0.50 g, 0.55 mmol) and *N*-methylglycine (0.10 g, 1.11 mmol) were dissolved in degassed and nitrogen flushed 1,2-dichlorobenzene (20 mL). After stirring at 150 °C for 18 h the polymer was recovered by precipitation in methanol (250 mL). Soxhlet-washing was then performed using acetone to yield a shiny black powder (yield = 67.9 %, 0.48 g). GPC (UV-visible) deconvolution indicated a trace of PCBM, i.e., around 0.3% by mass. Both OPCBMMB and PPCBMB were found to be soluble in a range of common organic solvents.

Scheme 1 shows the synthetic routes to the two PCBM-based materials, OPCBMMB and PPCBMB. As mentioned above, OPCBMMB is made using the ATRAP route, and typically results in very short oligomers (up to around 10 units or so). In this case, the methodology gave rise to extremely low molecular weight oligomers with between one and four repeating units and a high percentage (estimated around 35% by deconvolution of the GPC curve shown in Figure 2) of PCBM, because the reaction was performed on a relatively large scale with slow stirring.[35] In the case of the SACAP sample, the average number of repeating units was estimated to be around 27 by NMR.[24] The GPC in Figure 2 shows the profile of a polymer with a smooth curve due to their being much higher molecular weights present. The reader is referred to these two papers for more details on these materials.

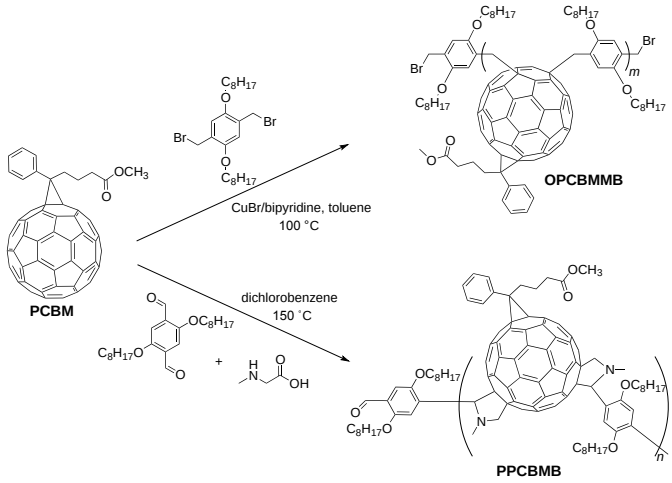

Scheme 1. Syntheses leading to OPCBMMB via the ATRAP route above, and PPCBMB by the SACAP method shown below.

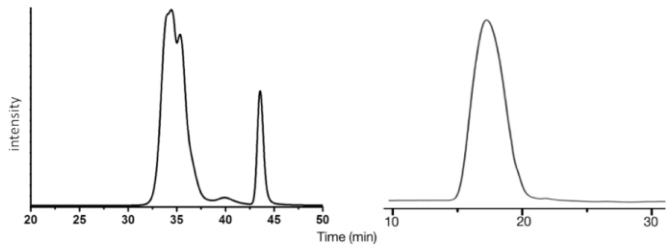

Figure 2. Left, GPC of OPCBMMB (THF, 30 °C, UV 300 nm; toluene flow marker at 43.5 mL),[35] and right, GPC of PPCBMB (THF, 30 °C, 330 nm) with a small bump at 21.85 min most likely due to trace PCBM.[24]

Density Functional Theory

Optimisations of geometries and energies were determined using Density Functional Theory (DFT) with the B3LYP exchange-correlation functional and 6-31G* basis set. Calculations were performed using Gaussian 09 program package[36]. DFT calculations were combined with Grimme's D3 method to account for longer-range dispersion interactions. The polarizable continuum model (PCM) was used in DFT calculus to model solvation effects.

Fabrication and characterization of Langmuir films

The PCBM-based materials were studied either alone or in mixtures with P3HT, and were were dispersed in either chloroform, xylene, or toluene each at a concentration of 0.2 mg mL^{-1}. The fullerenes were mixed at 1:1 %wt ratios with P3HT. UV-visible absorption spectroscopy measurements were performed in a Varian Cary 50 scan equipment, using the range from 300 nm to 900 nm. The UV-visible spectra for the PCBM-based materials solution were acquired in a quartz curvet. Solutions used to prepare the Langmuir films were diluted at 0.1 mg mL^{-1} to avoid saturation in the UV-Visible spectra.

Langmuir films were prepared using a Langmuir trough (model KSV 5000) with approximately 1350 mL of deionized water acquired from the Millipore Milli-Q water purification system (resistivity 18.2 MΩ cm). The spread solutions of the organic materials onto the aqueous subphase were compressed at 10 mm min^{-1} controlled by software, obtaining the surface pressure per area per monomer, i.e., the π-A isotherm.

The formation of Langmuir films was studied using the Brewster KSV NIMA micro-BAM angle microscope (field vision 3600 x 4000 μm^2) coupled to the Langmuir trough where images were taken at different surface pressures during film compression at the air/ultrapure water interface. For this study, we used xylene to solubilize the fullerene-based materials and chloroform to solubilize the mixtures of fullerene-based materials and P3HT.

Fabrication and characterization of Langmuir-Schaefer films

For the fabrication and characterization of the Langmuir-Schaefer (LS) films, the materials were first solubilized in xylene or chloroform (0.2 mg mL^{-1}). These solvents were chosen according to the study of the π-A isotherms, with two extremes being chosen, the solvent that better solubilizes the PCBM-based materials (xylene) and the regioregular P3HT (chloroform). The LS films were deposited onto indium-tin-oxide (ITO) substrates for optical and morphological measurements. The films were prepared using a 500 µL of solution (0.2 mg mL^{-1}) spread above the aqueous subphase and kept at a constant pressure of 20 mN m^{-1} while obtaining 15 LS layers onto ITO substrates.

The LS films were characterized by UV-visible absorption spectroscopy using the same equipment and wavelength range as described for the materials in solution. Contact mode atomic force microscopy (AFM) measurements were performed on the films (30 × 30 μm^2 area) to obtain information on nanoscale morphology. The equipment used for this characterization was the Nanosurf EasyScan 2 Microscope. The images obtained were treated and analyzed using the Gwyddion software (version 2.41). Raman spectra were acquired using a Renishaw micro-Raman spectrograph, model in-Via, equipped with a Leica microscope, laser line at 514.5 nm, 1800 lines/mm grating, time exposition of 10 s with a 50× objective lens, and CCD detector. This arrangement of laser, lens, and optical pathway gives a spatial resolution of around 1 µm (spot diameter of the focused laser beam). The measurements were taken on the ITO for the PCBM-based materials both pure and in mixtures with P3HT.

Results and Discussion

Langmuir films

The study of PCBM and its derivatives by Langmuir techniques aims to characterize the nanostructure of the materials spread as very thin layers at a water-air interface. Figure 3 shows the surface pressure versus mean area isotherms (π-A) of PCBM, OPCBMMB,

and PPCBMB, all of them previously solubilized in either chloroform, toluene, or xylene (0.2 mg mL^{-1}). The three different solvents were used to study their influence on the formation of the Langmuir films. The use of different solvents changes the arrangement of molecules and can increase or decrease the size and number of aggregates according to their polarity. Nonpolar solvents are the most used to solubilize these materials (relative polarity: chloroform 0.259; toluene 0.099 and xylene 0.074).[37] The isotherms show a strong indication of the formation of a liquid expanded phase, suggesting that the PCBM-based materials form disordered aggregates onto the aqueous subphase.[38] Due to the strong interaction of the π-π bonds of these materials, the PCBM quickly aggregated, following its well-known behavior.[39,17,40,41] Also, PCBM exhibited a lower molecular area than the other materials (OPCBMMB and PPCBMB) regardless of the solvent. The calculated molecular areas, following well-established methods,[42,43] are detailed in Table 1.

Table 1. Area per molecule (Å²) for the PCBM-based pristine materials and in mixtures with P3HT previously solubilized in different solvents. The increments in the area (%) were calculated from the pristine and mixed materials ratios.

	Chloroform			Toluene			Xylene		
	Pristine	P3HT	%	Pristine	P3HT	%	Pristine	P3HT	%
PCBM	23	25.1	9↑	9	29.2	224.4↑	12.4	27.1	118.5↑
OPCBMMB	128.5	69.8	45.7↓	66.7	75.7	13.4↑	75.2	68.9	8.37↓
PPCBMMB	123.3	77.2	37.3↓	106.2	89.3	15.9↓	89	80.6	9.4↓

According to the literature, the cross-surface area of PCBM is 100 Å², [41] and the estimated area from the π-A isotherms range from 9.0 to 23 Å², this means that there is a strong aggregation of PCBM regardless of the solvent used. These results may be due to a vertical build-up of the molecules in the air-water interface and therefore the apparent values are reduced. Similar result was presented by Liang *et al.*, who found a reduction in the area per molecule of C_{60} and stearic acid (SA), indicating that the film does not remain in a monomolecular layer attached to the water surface, but rather forms a multilayer film.[44] Interestingly, the mean area for the PCBM is similar to the values found in the literature when using chloroform, while from toluene and xylene solutions the areas are smaller (9 and 12.4 Å², respectively) suggesting that the water surfaces is less appealing to the PCBM when coming from these solutions. The solubilities of PCBM in chloroform, toluene and xylene are 28.8, 15.6, and 22.1 mg mL^{-1}, respectively, according to the literature.[45] Surprisingly, even when in good non-polar solvents such as xylene, one cannot ignore the possibility that PCBM readily forms very small nano-aggregates of several units which might not be visible using light-scattering. Given that C_{60} is known to rapidly form dimers and ether-bridges in air by way of oxidation, this result should not be so surprising.[46,47,48]

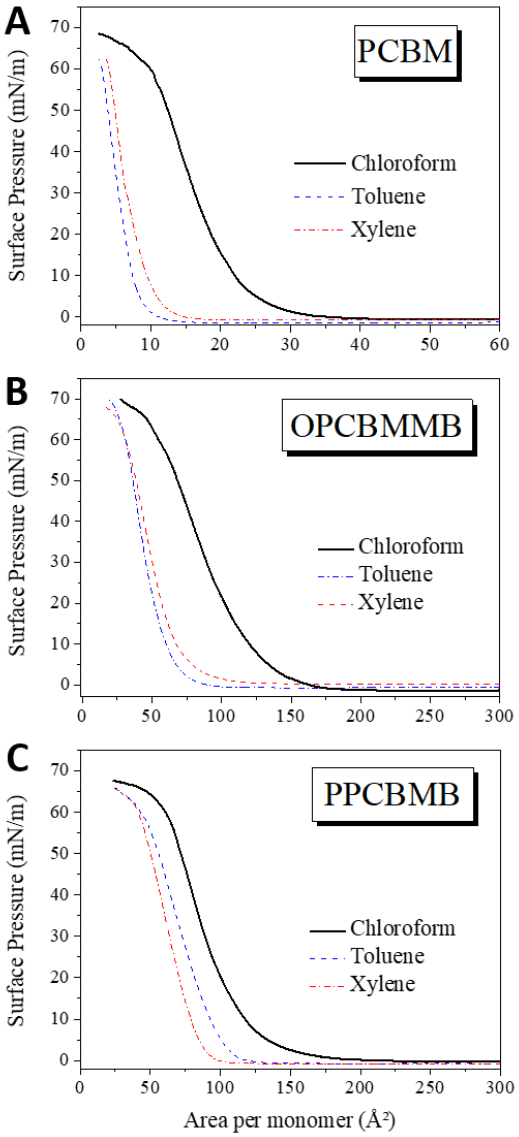

Figure 3. π-A isotherms of PCBM-based organic materials: a) PCBM, b) OPCBMMB and c) PPCBMB obtained from the materials solubilized in three different solvents (chloroform, toluene and xylene).

According to DFT/6-31+G* results presented in Figure 4, OPCBMMB and PPCBMB have structural differences: i) PPCBMB has an elongation in the 'X' direction of about 15% compared to OPCBMMB; ii) in the 'Z' direction, the OPCBMMB has a strong shortening about 20% compared to PPCBMB; and finally iii) the length in the 'Y' direction is basically the same for both monomers. Table 2 presents the areas of the monomers calculated based on the DFT results. We found that the calculated molecular areas are all higher than the ones estimated in the π-A isotherms of Figure 3, indicating that both materials aggregate in the Langmuir trough. In spite of that, the areas obtained by DFT are smaller in 'YZ' and 'XZ' direction than in 'XY', which suggests an orientation closer to a 'YZ' or 'XZ' configuration against the air-water interface. Another important point is the volume occupied by these materials, the OPCBMMB is 33% smaller than the PPCBMB, which is a significant difference. These theoretical results are in agreement with the experimental observations reported in Figure 3 and Table 1.

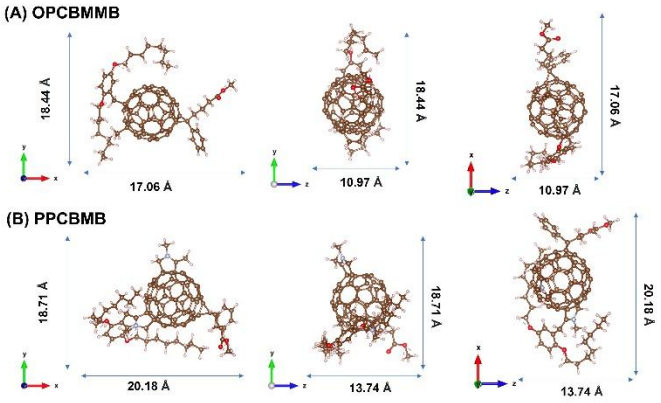

Figure 4. Theoretical model of the disposition of (a) OPCBMMB and (b) PPCBMB monomers in different orientations obtained by DFT.

Table 2. Areas and volumes of C_{60}, PCBM, OPCBMMB and PPCBMB monomers

	structural parameters (Å)			area in different orientations (Å²)			volume (Å³)
Materials	X	Y	Z	X.Y	Y.Z	X.Z	X.Y.Z
C_{60}	7.02	6.90	6.88	48.4	47.5	48.3	333.2
PCBM	14.79	9.82	6.96	145.2	68.4	102.9	1010.9
OPCBMMB	17.06	18.44	10.97	314.6	202.3	187.1	3451.0
PPCBMB	20.18	18.71	13.74	377.6	257.1	277.3	5187.8

extracted by theoretical DFT modelling (see text for details).

Complementary calculations were carried out under an implicit model of the solvent (PCM model) making it possible to implicitly average the degrees of freedom of the solvent and to treat the electrostatic interactions (generally dominant in the solvation) for C_{60}, PCBM, OPCBMMB and PPCBMB systems (see Supplementary Information). These new calculations show that neither the volumes nor the calculated surfaces are modified whatever the considered solvent (see tables S1, S2 and S3). These results reveal important information i.e., that it is not the electrostatic interactions that govern the behavior of the PPCBMB and OPCBMMB molecules in the solutions in our experiments as toluene, xylene and chloroform all have similar dielectric constants). The origin of the observed differences between the PCM calculations and the experiments is, therefore, to be found elsewhere and in particular in the absence of explicit consideration of the first solvation layer in the PCM model. Because of its smaller size and the presence of chlorine, chloroform is, of the three solvents used in this work, the one that will most likely favor the setting up of these interactions by inserting itself more easily into the structures of the PPCBMB and OPCBMMB molecules, automatically increasing the volume and the surfaces of these systems.

While these results are interesting, PCBM-based materials are rarely used by themselves. Therefore, we studied the behavior of their mixtures with P3HT (1:1), and the π-A isotherms are presented in Figure 5. The areas per monomers were calculated from the isotherms for the PCBM-based materials mixed with P3HT using the same aforementioned method, and the estimated values are also presented in Table 1 to easily compare them. The addition of P3HT probably influences the interaction and organization of these materials at the air-water interface, consequently altering the estimated areas per molecule/monomer. Figure 5(a) shows the π-A isotherm of pure P3HT, and the estimated area per monomer is ~ 4.7 Å^2, similar to the values found in the literature.[49]

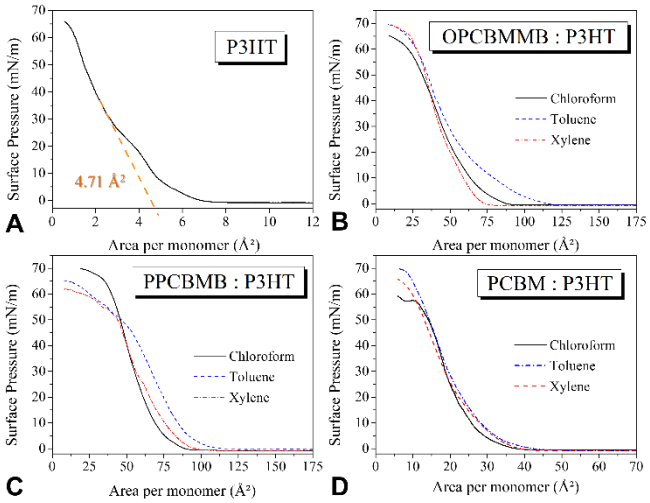

Figure 5. π-A isotherms of PCBM-based materials mixed with P3HT: a) PCBM:P3HT, b) OPCBMMB:P3HT and c) PPCBMB:P3HT obtained for the materials previously solubilized in chloroform, toluene and xylene. d) π-A isotherm for P3HT previously solubilized in chloroform.

From the estimated areas (Table 1), for chloroform solutions of PCBM, there is a small difference in the molecular areas for PCBM alone (23 Å²) and PCBM:P3HT mixture (25.1 Å²). There is an increase in the estimated area per monomer of PCBM:P3HT when previously solubilized in toluene and xylene, possibly related to a greater diffusion of the PCBM with P3HT due to the higher solubility of PCBM in those solvents. For OPCBMMB and PPCBMB there is a clear and definite decrease in the molecular areas by about 45% and 37% when mixed with P3HT in chloroform solutions. This means that in these chloroform solutions the OPCBMMB and the PPCBMB are aggregating and forming more vertical-like structures away from the water surface. This process is strongest in the case of OPCBMMB solubilized in chloroform. This might be for two reasons; first, it has a lower molecular weight and therefore can be expected to reorganize more easily, and also PPCBMB carries more polar amine groups, which might favor its interaction with the water surface. Using the other solvents (toluene and xylene) to combine the PCBM-based materials with P3HT, we observed more mildly changes in the estimated area per monomer. For instance, previously solubilized in toluene, the OPCBMMB had an increase in the estimated area per monomer of 13% while for the PPCBMB it decreased by about 16%. For xylene, we found the smallest decrease in the estimated areas, about 8% and 9%, for OPCBMMB and PPCBMB, respectively. Prior work has shown that mixed films of P3HT and fullerene-derivatives can actually promote stronger interactions between fullerenes, leading to reduced values for molecular areas.[50,51]

Finally, we can consider the isotherms in Figure 6, where we see the same data from Figures 3 and 5 presented in a different

manner. Here we have the curves for all materials in all solvents. However, we have now added data, in the black line in each plot, that shows the actual effective surface area calculated supposing that the surface of the Langmuir trough was made of P3HT molecules instead of water. If the modified curves are far from the P3HT isotherm, then obviously it is the result of a material that is not just P3HT and then the supposition is incorrect. Since the black curves in the isotherms of Figure 6 represent shifts from the isotherms of mixed materials (red curves) towards the response of P3HT, these results indicate that the footprint on the water is determined by P3HT. Therefore P3HT monomers are mainly underlying PCBM, OPCBMMB and PPCBMB in the Langmuir trough. Additionally, we can see that the modified curves of all mixed materials (black lines) previously solubilized in chloroform are less close to the P3HT isotherm (pink lines) than when solubilized in toluene or xylene. This means that to some extent there is greater mixing of P3HT and the fullerene-based materials in chloroform than in toluene or xylene. Chloroform is known to be an excellent solvent for P3HT, taking on more than 30 mg.mL^{-1}, whereas toluene and xylene are less powerful solvents, managing only around 7 and 3 mg.mL^{-1}, respectively, thus explaining this occlusion.[49]

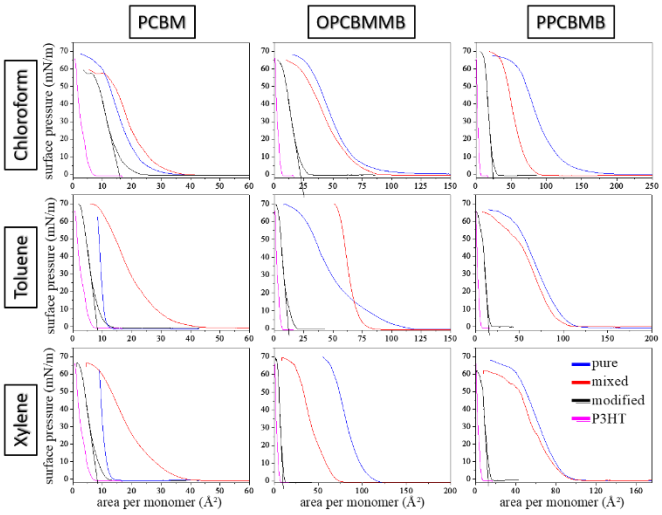

Figure 6. π-A isotherms for Langmuir films of PCBM, OPCBMMB, PPCBMB and P3HT either pure or mixed (0.2 mg mL^{-1}) and cast from Chloroform, Toluene or Xylene solutions. The black lines represent the isotherms obtained when assuming the surface is formed by P3HT monomers instead of water molecules.

To summarize, we can attribute the influence of the solvents in the isotherms and therefore in the estimated areas for the PCBM-based materials mixed with P3HT (1:1) to their solubilization power. P3HT presents better chloroform solubilities, thus increasing the P3HT interaction with fullerenes.[49]

BAM images of the fullerene-based materials both pure and mixed with P3HT are presented in Figures 7 and 8, respectively. The images show us four situations for each material: a) the scattering stage, where it is already possible to visualize some clusters of materials; b) all material solution has been scattered and then is allowed 15 minutes for solvent evaporation; c) when the barriers compress the material at a pressure of 15 mN.m^{-1} in which we verify the formation of some domains and the aqueous phase is still observed (darker areas); and d) when the pressure reaches 20 mN.m^{-1}, we observe that the aggregates of the materials form packed structures covering the whole areas in the images.[52] The strong tendency of these materials to aggregate is clear in the images, indicating the formation of multilayers instead of forming a true monolayer.

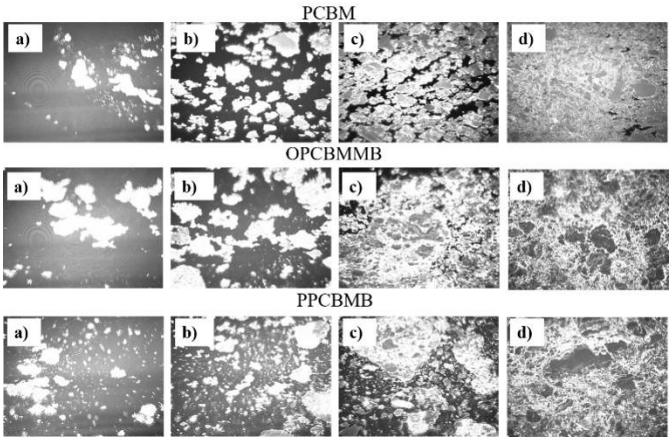

Figure 7. Brewster Angle Microscopy images for PCBM, OPCBMMB and PPCBMB previously solubilized in xylene: a) during the process of solution spreading, b) after solvent evaporation, c) at 15 mN.m^{-1} and d) 20 mN.m^{-1}. The images were obtained with 3600 x 4000 μm^2 field vision.

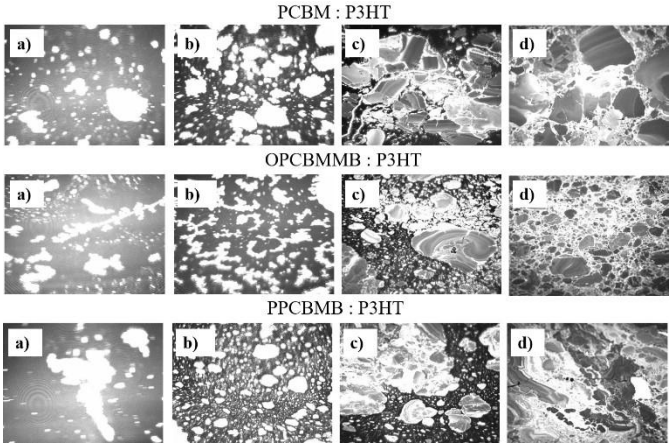

Figure 8. Brewster Angle Microscopy images for PCBM-based materials mixed with P3HT previously solubilized in chloroform: a) spreading solution, b) solvent evaporation, c) at 15 mN.m^{-1} and d) 20 mN.m^{-1}. The images were obtained with 3600 x 4000 μm^2 field vision.

In general, the formation of aggregates and material domains is very similar in the three derivatives PCBM, PPCBMB and OPCBMMB indicating that aggregation is a common factor for these materials.[53,54] For the pure materials at 20 mN.m^{-1} (Figure 7(d)) there are larger domains (darker regions) for the PPCBMB and OPCBMMB, the ones that showed the larger areas in the isotherms, while for PCBM we have a more uniform film indicating smaller domain areas, which is in agreement with the estimated areas from the isotherms.

The formation of these aggregates for the mixed materials is also visualized and clearly shows a close mixture of two phases with separate domains. By increasing the surface pressure of the aqueous subphase (15 $mN.m^{-1}$ and 20 $mN.m^{-1}$) lamellar structures are observed for the three materials (Figure 8(c) and (d)). When we compare with the mixed material images, we notice the difference in the formation of these domains, with more distinct phases (black, white and dark gray region), this refers to the way these materials are organizing themselves at the air-water interface. The addition of P3HT causes these materials to overlap each other (white and gray regions). A possible interpretation is that P3HT is upon almost the entire aqueous surface with fullerene-based materials clustering as islands on top of the P3HT layer.[55,56] Therefore, from the π-A isotherms of the Langmuir films and the BAM images, we proposed a configuration of the materials on the aqueous surface of the Langmuir trough. Figure 9 shows the proposed structures for fullerene-based materials, both pure and mixed with P3HT, arranged in the air/water interface.

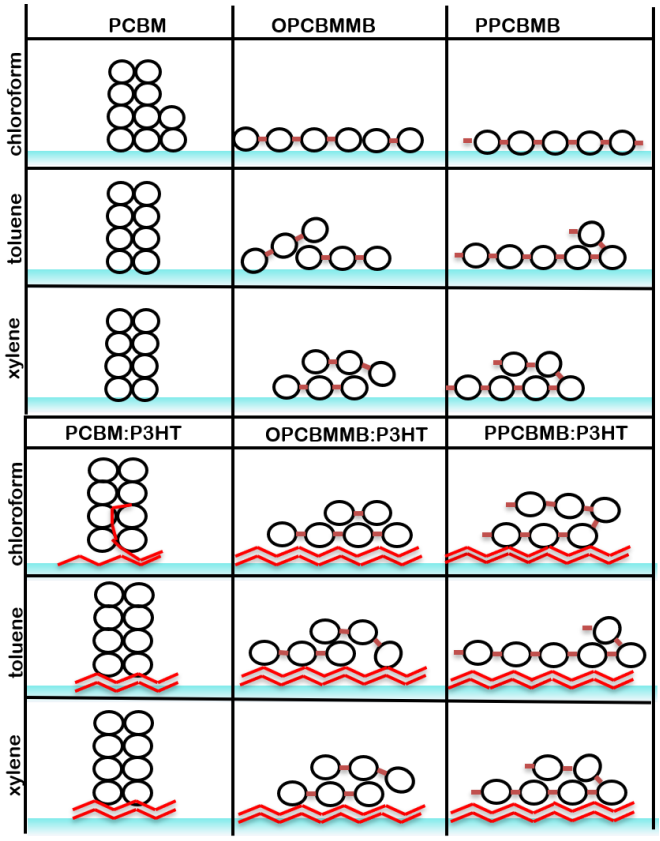

Figure 9. Proposed structures for the fullerene-based materials, both pure and mixed with P3HT, on the water surface of the Langmuir trough.

It was not possible to deposit the Langmuir layers onto solid substrates by Langmuir-Blodgett technique (vertical deposition) because all the PCBM-based materials were unable, at least in our hands, to form stable monolayers or multilayers at an air-water interface. However, it was much more feasible to employ a horizontal deposition, i.e., the Langmuir-Schaefer technique,[57,58] to deliver characterizable films on solid substrates.

UV-Visible spectroscopy

Figure 10 shows the UV-visible absorption spectra for PCBM-based materials both pure (a, c and e) and mixed with P3HT (b, d and f). There is a clear similarity between the OPCBMMB and PCBM spectra. The synthesis of the OPCBMMB in the work of Ramanitra *et al.*[23], shows that the large proportion of PCBM remaining in the OPCBMMB material may overlap many of the electronic properties of oligomers. The similarity in these spectra indicates that additional peaks due to asymmetric additions during ATRAP did not occur. This suggests that the ATRAP method occurred at a specific position (1,4-phenylene on the C_{60} sphere), producing symmetrical products with similar properties to PCBM.[35,30,59]

The UV-vis spectra obtained for the PCBM-based materials solubilized in different solvents (Figures 10 a, c and e) show the characteristic absorbance of fullerene derivatives (300-450 nm) for excited singlet transitions.[60,61] This is clearly seen for PCBM and OPCBMMB (Figures 10 a and c, respectively) with two major peaks at 330 nm for the sphere (C_{60}) and 430 nm for the connections between the six-membered rings [6-6].[62,30,63] The use of different solvents such as chloroform, toluene and xylene showed differences only in the absorbance intensities and not in the wavelength of their peak. The relative absorbances of the peaks at 430 and 330 nm decreased for the chloroform solutions of PCMB and OPCBMMB (black line) in comparison to the solutions of toluene and xylene (red and blue lines). According to the literature,[64,65] this may be related to increased aggregation in the chloroform solution of both materials. This fact is also verified for PPCBMB (Figure 10 e), in which there is a decrease in the relative intensity between the estimated maximum at 300 nm and the baseline of the chloroform solution when compared to the solutions of toluene and xylene. This shows that the solvent influences not only the aggregation as shown in the study of the π-A isotherms, but also the absorption spectra. A similar outcome was described by Bensasson *et al.*,[64] who found that the formation of aggregates depends mainly on the polarization of the solvent and has a direct relationship to the maximum absorption.[24,66] Regardless of the solvent used, the UV-Vis spectra of the PPCBMB solutions show a blue-shift (300 nm) in relation to the maximum presented by the PCBM and OPCBMMB (330 nm). This fact can be attributed to a greater break in the fullerene aromaticity during synthesis with the SACAP method.[24,67]

For PCBM and OPCBMMB there is a small shift of the peaks from ~330 in solution to ~335 nm as LS films. It was also observed in the LS films an intensity increase of the band at ~400-500 nm. These changes may be related to the formation of a packed structure of the materials as solid films, which reflects in the absorption profile. We can also speculate that the functionalization of PCBM with 1,4-phenylene groups is more strongly evidenced by the organization of the film,[60,61] permitting an increase in the absorbance of the related band.

The UV-vis absorption spectra of PCBM-based materials mixed with P3HT are shown in Figures 10 b, d and f for PCBM, OPCBMMB and PPCBMB, respectively. We see characteristic absorptions related to P3HT at ~450 nm for the solutions and a redshift to ~515 nm for the LS films, probably related to a higher packing and ordering of the molecules when processed as thin films.[68,69] The packing of the P3HT thiophene ring causes this displacement

containing two vibronic resolution peaks and one shoulder, implying greater conjugation length. These vibrational levels of the π-π* transition have absorption maxima close to 515 nm, 550 nm, and 600 nm respectively, and have a relationship to interlayer interactions of films.[70,60,71] Moreover, the peaks previously attributed to the fullerenes are also present in the UV-vis spectra of the mixed materials, either in solution or processed as LS films. For the films, the peak undergoes a small redshift of approximately 5 nm, and this deviation may be associated with a general ordering degree and a longer conjugation length, showing that the interaction between the two materials (PCBM derivatives and P3HT) was just a sum of their individual peaks.[72]

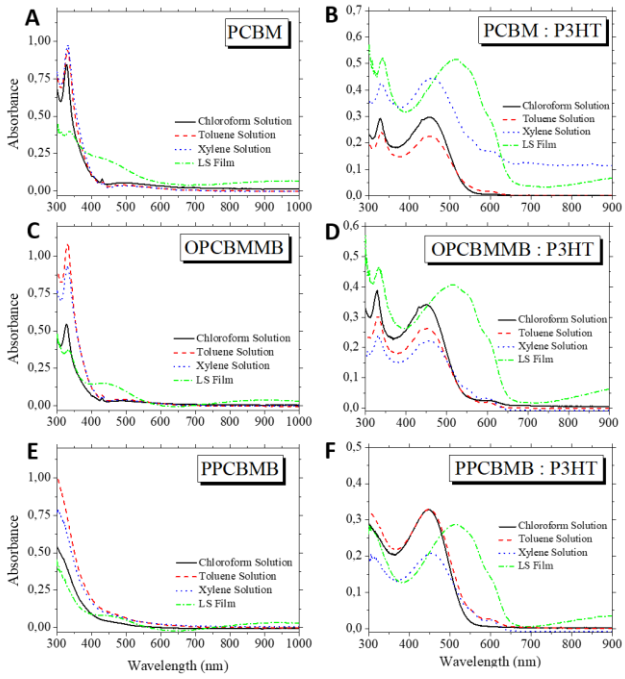

Figure 10. UV-visible spectra for PCBM-based materials a), c) and e) for pure solutions, and b), d) and f) for mixed solutions with P3HT; and all their respective LS films.

Atomic Force Microscopy

To evaluate the nanoscale morphologies of materials on solid substrates, AFM measurements were performed, obtaining topographic images of LS films of PCBM, OPCBMMB and PPCBMB, both pure and mixed with P3HT. Figures 11 and 12 show the AFM images for the LS films fabricated from the materials solutions in chloroform and xylene, respectively. The roughness values obtained from these images are shown in Table 3.

The images presented in Figure 11 reveal that the LS films of the fullerene-based materials have more agglomerates and higher roughness compared to their equivalent when mixed with P3HT. The PCBM showed the highest roughness among the materials solubilized in chloroform, which decreases drastically when mixed with P3HT (~81%). We found that when using the chloroform solvent, mixed materials (fullerenes:P3HT (1:1)) exhibited a reduction in their roughness compared to pure ones, which may be associated with a greater diffusion of P3HT among fullerenes. The LS films fabricated from OPCBMMB:P3HT and PPCBMB:P3HT solubilized in chloroform presented similar roughness, and the images of the mixed films revealed some island domains. This can be associated with the close mixture of two phases (polymer and fullerene), as seen in the images obtained from the BAM technique (Figure 8).[55]

Figure 12 presents the equivalent topographic AFM images of Figure 11, here with the materials cast from xylene solutions instead of chloroform. The images reveal surfaces with more agglomerates for the mixed films (fullerenes:P3HT), revealing higher roughness compared to LS films of pure fullerene-based materials. The highest roughness was obtained for the film of PCBM:P3HT (144 nm), which showed an increase of ~128% compared with the LS film of pure PCBM. PPCBMB showed the lowest roughness among the three materials, considering both pure and mixed with P3HT. However, the pattern is the same as the observed for PCBM and OPCBMMB, in which PPCBMB shows an increase in roughness (136%) when mixed with P3HT.

Therefore, according to the AFM results, the solvent used implies changes in the morphology of LS films of the fullerene-based materials both pure and in mixtures with P3HT. To summarize, the roughness is lowest when using xylene solvent for the pure materials, while for the mixed materials, chloroform resulted in the lowest roughness. This is associated with the solubility of the materials since it interferes with the organization of the molecules in the aqueous sub-phase of the Langmuir trough. This result is relevant since films of fullerenes mixed with P3HT show improvements in conductivity/mobility, according to the literature,[73,74,75] and these improvements may be related to the fact that mixed films from P3HT show higher homogeneity and lower roughness, at least when prepared with chloroform.

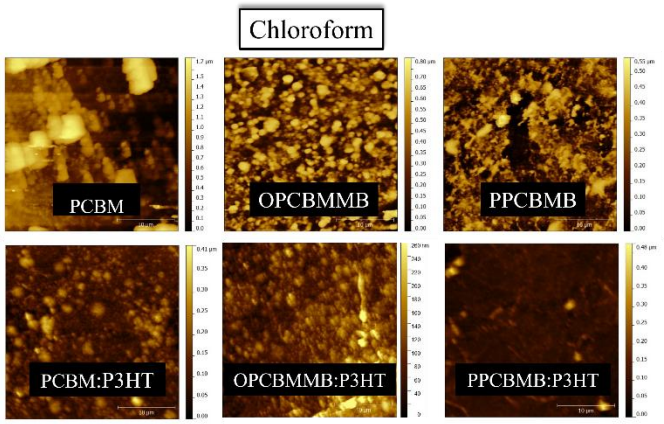

Figure 11. AFM images of LS films of pure PCBM derivatives and mixed with P3HT, obtained from chloroform solutions. The images were obtained with 30 × 30 μm^2 area.

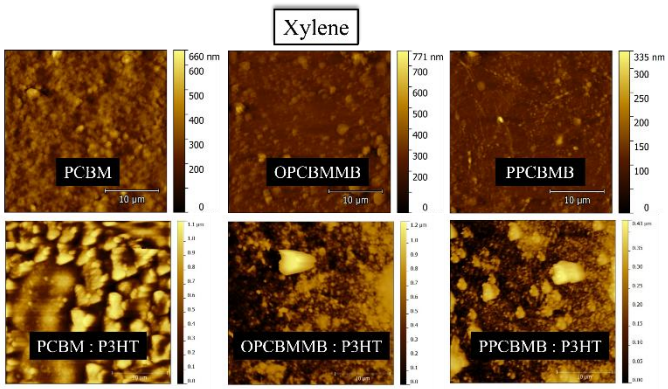

Figure 12. AFM images of LS films of pure PCBM derivatives and mixed with P3HT, obtained from xylene solutions. The images were obtained with 30 × 30 μm^2 area.

Table 3: Roughness values (nm) for LS films of PCBM-based materials and in mixtures with P3HT. Percentage of increase or decrease of roughness when mixed P3HT.

	chloroform			xylene		
	pristine	P3HT	%	pristine	P3HT	%
PCBM	268.0	50.5	81.15↓	63.12	144	128.13↑
OPCBMMB	43.0	34.7	19.3↓	53.64	103.0	92.0↑
PPCBMB	42.6	34.6	18.7↓	18.97	44.8	136.16↑

Raman Spectroscopy

Raman microscopy measurements were performed to obtain information at micrometer scale on the homogeneity and distribution of components within the LS films, with information from different regions of the pure and mixed films. Figures 13 and 14 show a photoluminescence spectra signal that was detected from the pure LS films of the PCBM-based materials solubilized in xylene and chloroform, respectively. Similar photoluminescence spectra are found in the literature for PCBM-based materials.[76,77,78] The different regions selected show us changes in relative intensities, meaning different quantities of material for each region. Previously shown BAM and AFM images can be used to corroborate the influence of the aggregates on the film's roughness and on the multilayers formed by the aggregation of the materials in Langmuir and LS films, respectively.

The pure PCBM and OPCBMMB films prepared from xylene solutions (Figure 13) show similarities between them. These materials present a great difference in their relative intensities. The regions where the presence of the material is higher (PCBM - black circle and OPCBMMB - blue circle), and regions where the presence of the material is lower (PCBM - red circle and OPCBMMB - red and black circle), indicates that the film manufactured with these materials are not homogeneous at the micrometer scale, agreeing with the roughness obtained by the AFM technique, in which these materials showed the highest roughnesses. When we analyze the PPCBMB, it shows the lowest roughness of the three materials and also a close pattern in Raman intensity, i.e., there is a low variation in the intensity for the three regions, indicating a more homogeneous LS film. The behavior repeats when we use the chloroform solvent, as shown in Figure 14. PCBM and OPCBMMB show a greater difference in their relative Raman intensities, compared to PPCBMB. The regions where the presence of the material are higher (PCBM - red circle and OPCBMMB - red circle), and regions where the presence of the material are lower (PCBM - black circle and OPCBMMB - black circle) show significant differences in the Raman intensities, suggesting that the amount of material varies according to the position, which is in accordance with the obtained roughness values.

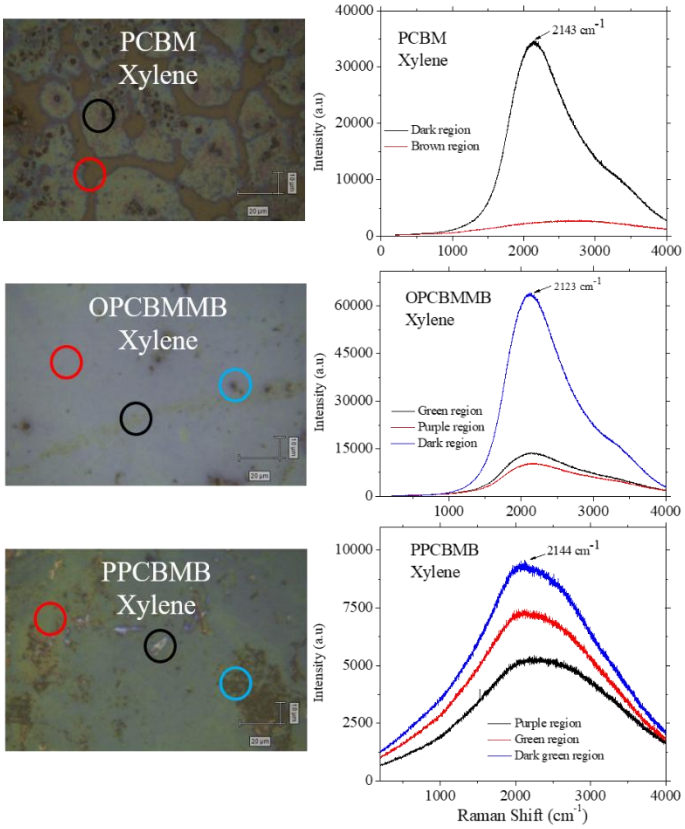

Figure 13. Photoluminescence spectra for LS films of PCBM-based materials prepared from xylene solutions. The images were obtained with 100 × 200 μm^2 area.

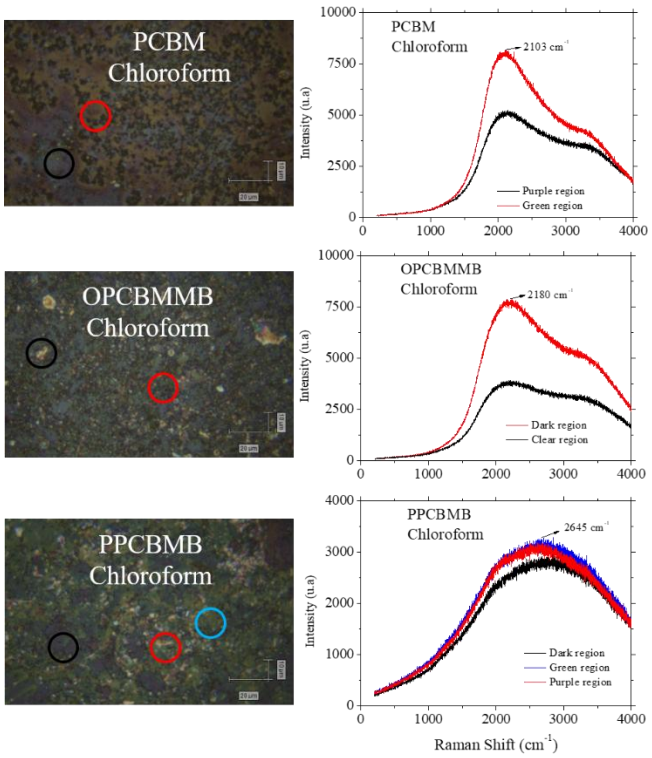

Figure 14. Photoluminescence spectra for LS films of PCBM-based materials prepared from chloroform solutions. The images were obtained with 100 × 200 μm^2 area.

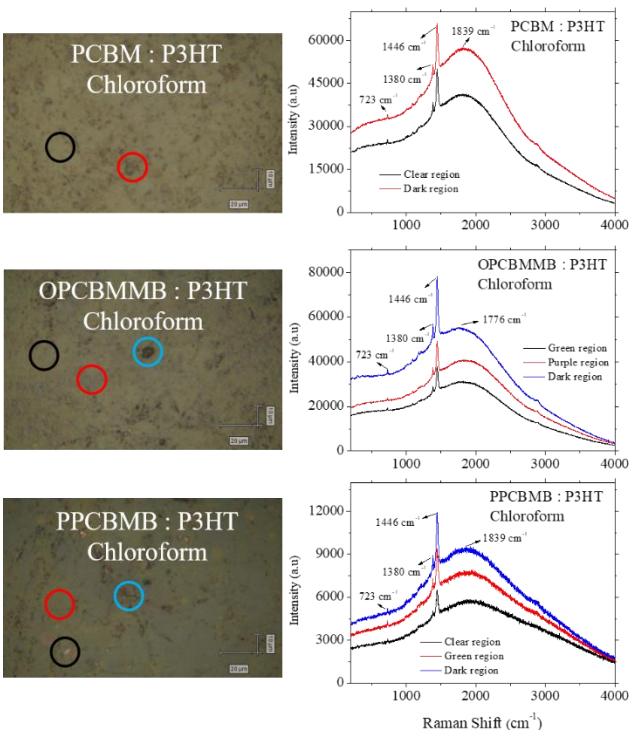

Figure 15. Raman spectra for LS films of PCBM-based materials mixed with P3HT previously solubilized in chloroform. The images were obtained with 100 × 200 μm^2 area.

Figures 15 and 16 show the Raman spectra of mixed films (P3HT: PCBM-based materials (1:1)) solubilized in chloroform and xylene, respectively. The strong photoluminescence signal characteristic of the fullerene-based materials is maintained for all samples. The presence of P3HT shows two peaks at 1446 and 1390 cm^{-1} that are associated with the stretching modes of C=C and C-C[56], respectively, and a third one at 727 cm^{-1}, associated with deformation of the C-S-C thiophene ring [79,80], seen in films solubilized with chloroform. The high intensity at 1446 cm^{-1} indicates an increase in the crystallinity of the P3HT polymer and the extension of the effective length of the conjugation along the chain[81], which is often used to indicate the ordering of the film[82,71]. This suggests that mixed LS films solubilized in chloroform are ordered and corroborate with the results observed in the UV-vis spectra.

When changing the solvent to xylene (Figure 16), the peaks corresponding to P3HT are less evident, i.e., their relative intensities decrease. We found that for the PCBM:P3HT the peak at 1446 cm^{-1} has its relative intensity below the PCBM at 2116 cm^{-1}. The Raman spectrum for OPCBMMB:P3HT, despite exhibiting a higher relative maximum of P3HT in relation to the fullerene photoluminescence band, its relative intensity was much lower when using xylene compared to the spectra obtained for the LS film of the same materials prepared from chloroform solution. This is associated with the lower solubility of P3HT with the xylene, increasing the agglomerates as seen previously in the AFM measurements and, consequently, decreasing their organization. The effect, however, is not evident when we observe the PPCBMB:P3HT having its relative intensities similar to the result obtained for the LS film prepared from chloroform solution. Therefore, PPCBMMB mixed with P3HT proved to be suitable for the two solvents used providing a more homogeneous film.

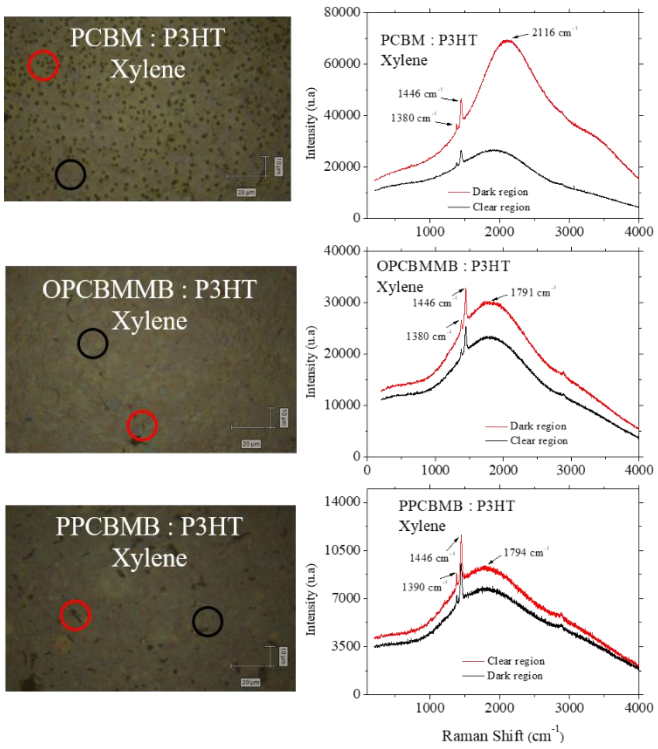

Figure 16. Raman spectra for LS films of PCBM-based materials mixed with P3HT previously solubilized in xylene. The images were obtained with 100 × 200 μm^2 area.

According to Motaung *et al.,* the mixture of P3HT and PCBM causes a disorder in the P3HT chains due to the diffusion of the PCBM molecules, forming clusters, leading to phase separation (P3HT and PCBM)[71]. There is a huge difference between the images acquired with Raman microscope for both pure and mixed LS films. The distribution of agglomerates is the main difference between them, with agglomerates randomly distributed in the pure films, while for the mixed films there is a more uniform distribution of them.

The regions observed in the three mixed materials studied (PCBM:P3HT and PCBM-based materials:P3HT) (red, blue and black), although the images show that the regions have different morphological aspects, the Raman spectra are demonstrating that chemically the regions are analogous and the two mixed materials (PCBM-based materials and P3HT) are present in all. In general, the spectra of the mixed materials are simple overlaps of the individual spectra, confirming no chemical interactions, regardless of the solvent used.

Conclusions

This study has shown it is possible to successfully fabricate Langmuir and Langmuir-Schaefer films of PCBM and PCBM-based oligomers and polymers, both pure and mixed with P3HT, comparing their organization, roughness, and optical properties. With the Langmuir films, it was possible to estimate the area of the molecules and visualize their aggregation through BAM images, establishing a relationship between the area occupied by these materials and the solvent used. According to the results, the solvent used implies changes in the morphology of Langmuir and LS films of the PCBM-based materials both pure and in mixtures with P3HT. To summarize, the roughness is lower when using xylene with pure materials, most likely due to the slow evaporation of xylene, while with mixed materials, the lower roughness was obtained using chloroform which permitted a greater intermixing of the P3HT and PCBM or PCBM derivatives. This is associated with the solubility of the materials since it interferes with the organization of the molecules in the aqueous sub-phase of the Langmuir trough. All characterization techniques (UV-visible absorption spectroscopy, AFM and Raman) corroborate that the use of chloroform significantly reduced the roughness of LS films mixed with P3HT and also presented a higher ordering compared to films prepared with xylene solutions. Moreover, the size domains are affected by the solvent used and for each PCBM-based material. Therefore, the main conclusion is if you want to make a solid film of PCBM-based materials with P3HT then a good solvent, such as chloroform has considerable impact, but only when used with mixtures.

Conflicts of interest

There are no conflicts to declare.

Acknowledgements

This research was financially supported by the Brazilian agencies São Paulo Research Foundation (FAPESP, nº 2020/12060-1), National Council for Scientific and Technological Development (CNPq), and Coordenação de Aperfeiçoamento de Pessoal de Nível Superior (CAPES, nº 88887.583380/2020-00).

References

1 K. Jiang, Q. Wei, J. Y. L. Lai, Z. Peng, H. K. Kim, J. Yuan, L. Ye, H. Ade, Y. Zou and H. Yan, Alkyl Chain Tuning of Small Molecule Acceptors for Efficient Organic Solar Cells, *Joule*, 2019, **3**, 3020–3033.

2 J. Yuan, Y. Zhang, L. Zhou, G. Zhang, H.-L. Yip, T.-K. Lau, X. Lu, C. Zhu, H. Peng, P. A. Johnson, M. Leclerc, Y. Cao, J. Ulanski, Y. Li and Y. Zou, Single-Junction Organic Solar Cell with over 15% Efficiency Using Fused-Ring Acceptor with Electron-Deficient Core, *Joule*, 2019, **3**, 1140–1151.

3 Q. Liu, Y. Jiang, K. Jin, J. Qin, J. Xu, W. Li, J. Xiong, J. Liu, Z. Xiao, K. Sun, S. Yang, X. Zhang and L. Ding, 18% Efficiency organic solar cells, *Sci. Bull.*, 2020, **65**, 272–275.

4 L. Meng, Y. Zhang, X. Wan, C. Li, X. Zhang, Y. Wang, X. Ke, Z. Xiao, L. Ding, R. Xia, H.-L. Yip, Y. Cao and Y. Chen, Organic and solution-processed tandem solar cells with 17.3% efficiency, *Science (80-.).*, 2018, **361**, 1094–1098.

5 A. Grebinyk, S. Prylutska, S. Grebinyk, Y. Prylutskyy, U. Ritter, O. Matyshevska, T. Dandekar and M. Frohme, Complexation with C60 Fullerene Increases Doxorubicin Efficiency against Leukemic Cells In Vitro, *Nanoscale Res. Lett.*, 2019, **14**, 61.

6 J. Shi, X. Yu, L. Wang, Y. Liu, J. Gao, J. Zhang, R. Ma, R. Liu and Z. Zhang, PEGylated fullerene/iron oxide

nanocomposites for photodynamic therapy, targeted drug delivery and MR imaging, *Biomaterials*, 2013, **34**, 9666–9677.

7 R. Bakry, R. M. Vallant, M. Najam-ul-Haq, M. Rainer, Z. Szabo, C. W. Huck and G. K. Bonn, Medicinal applications of fullerenes., *Int. J. Nanomedicine*, 2007, **2**, 639–49.

8 H. C. Wong, Z. Li, C. H. Tan, H. Zhong, Z. Huang, H. Bronstein, I. McCulloch, J. T. Cabral and J. R. Durrant, Morphological Stability and Performance of Polymer–Fullerene Solar Cells under Thermal Stress: The Impact of Photoinduced PC 60 BM Oligomerization, *ACS Nano*, 2014, **8**, 1297–1308.

9 M. Campoy-Quiles, T. Ferenczi, T. Agostinelli, P. G. Etchegoin, Y. Kim, T. D. Anthopoulos, P. N. Stavrinou, D. D. C. Bradley and J. Nelson, Morphology evolution via self-organization and lateral and vertical diffusion in polymer:fullerene solar cell blends, *Nat. Mater.*, 2008, **7**, 158–164.

10 S. H. Park, A. Roy, S. Beaupré, S. Cho, N. Coates, J. S. Moon, D. Moses, M. Leclerc, K. Lee and A. J. Heeger, Bulk heterojunction solar cells with internal quantum efficiency approaching 100%, *Nat. Photonics*, 2009, **3**, 297–303.

11 J. C. Hummelen, B. W. Knight, F. LePeq, F. Wudl, J. Yao and C. L. Wilkins, Preparation and Characterization of Fulleroid and Methanofullerene Derivatives, *J. Org. Chem.*, 1995, **60**, 532–538.

12 F. W. Francesco Giacalone, Nazario Martin, *Fullerene Polymers*, Wiley, Weinheim, Germany, Wiley-VCH., 2009.

13 M. D. Tzirakis and M. Orfanopoulos, Radical Reactions of Fullerenes: From Synthetic Organic Chemistry to Materials Science and Biology, *Chem. Rev.*, 2013, **113**, 5262–5321.

14 W. Śliwa, Cycloaddition Reactions of Fullerenes, *Fuller. Sci. Technol.*, 1995, **3**, 243–281.

15 W. E. Billups, Fullerenes: Chemistry and Reactions By Andreas Hirsch and Michael Brettreich (Friedrich Alexander University of Erlangen-Nuremberg). Wiley-VCH Verlag GmbH & Co. KGaA: Weinheim, Germany. 2005. xviii + 423 pp. $180.00. ISBN 3-527-30820-2., *J. Am. Chem. Soc.*, 2005, **127**, 11876–11876.

16 B. Gholamkhass, T. J. Peckham and S. Holdcroft, Poly(3-hexylthiophene) bearing pendant fullerenes: aggregation vs. self-organization, *Polym. Chem.*, 2010, **1**, 708.

17 C. Long, Y. Xu, C. Zhu, D. Zhu, F. Desorption and M. Spectrometry, Tem Study on Langmuir-Blodgett Films of two novel C60 Derivatives Chengfen Long, Yu Xu, Changcheng Zhu and Daoben Zhu Institute of Chemistry, Chinese Academy of Sciences, Beijing 100080, China, 1997, **101**, 439–442.

18 Y. Gao, Z. Tang, E. Watkins, J. Majewski and H. L. Wang, Synthesis and characterization of amphiphilic fullerenes and their Langmuir-Blodgett films, *Langmuir*, 2005, **21**, 1416–1423.

19 L. Robitaille and M. Leclerc, Synthesis, Characterization, and Langmuir-Blodgett Films of Fluorinated Polythiophenes, *Macromolecules*, 1994, **27**, 1847–1851.

20 B. Li, G. Sauvé, M. C. Iovu, M. Jeffries-EL, R. Zhang, J. Cooper, S. Santhanam, L. Schultz, J. C. Revelli, A. G. Kusne, T. Kowalewski, J. L. Snyder, L. E. Weiss, G. K. Fedder, R. D. McCullough and D. N. Lambeth, Volatile Organic Compound Detection Using Nanostructured Copolymers, *Nano Lett.*, 2006, **6**, 1598–1602.

21 J. A. Zasadzinski, R. Viswanathan, L. Madsen, J. Garnaes and D. K. Schwartz, Langmuir-Blodgett films, *Science (80-.).*, 1994, **263**, 1726–1733.

22 M. L. Braunger, P. Alessio, L. N. Furini, C. J. L. Constantino and C. A. Olivati, Influence of the Supramolecular Arrangement in the Electrical Conductivity of Poly(thiophene) Thin Films, *J. Nanosci. Nanotechnol.*, 2017, **17**, 460–466.

23 H. H. Ramanitra, H. Santos Silva, B. A. Bregadiolli, A. Khoukh, C. M. S. Combe, S. A. Dowland, D. Bégué, C. F. O. Graeff, C. Dagron-Lartigau, A. Distler, G. Morse and R. C. Hiorns, Synthesis of Main-Chain Poly(fullerene)s from a Sterically Controlled Azomethine Ylide Cycloaddition Polymerization, *Macromolecules*, 2016, **49**, 1681–1691.

24 M. Stephen, H. H. Ramanitra, H. Santos Silva, S. Dowland, D. Bégué, K. Genevičius, K. Arlauskas, G. Juška, G. E. Morse, A. Distler and R. C. Hiorns, Sterically controlled azomethine ylide cycloaddition polymerization of phenyl-C61-butyric acid methyl ester, *Chem. Commun.*, 2016, **52**, 6107–6110.

25 D. A. Loy and R. A. Assink, Synthesis of a fullerene C60-p-xylylene copolymer, *J. Am. Chem. Soc.*, 1992, **114**, 3977–3978.

26 A. Gügel, P. Belik, M. Walter, A. Kraus, E. Harth, M. Wagner, J. Spickermann and K. Müllen, The repetitive Diels-Alder reaction: A new approach to [60]fullerene maindashchain polymers, *Tetrahedron*, 1996, **52**, 5007–5014.

27 G. P. Miller, Reactions between aliphatic amines and [60]fullerene: a review, *Comptes Rendus Chim.*, 2006, **9**, 952–959.

28 S. Samal, B.-J. Choi and K. E. Geckeler, The first water-soluble main-chain polyfullerene, *Chem. Commun.*, 2000, 1373–1374.

29 R. C. Hiorns, E. Cloutet, E. Ibarboure, L. Vignau, N. Lemaitre, S. Guillerez, C. Absalon and H. Cramail, Main-Chain Fullerene Polymers for Photovoltaic Devices - Supporting Information, 2009, 1–12.

30 R. C. Hiorns, E. Cloutet, E. Ibarboure, A. Khoukh, H. Bejbouji, L. Vignau and H. Cramail, Synthesis of donor-acceptor multiblock copolymers incorporating fullerene backbone repeat units, *Macromolecules*, 2010, **43**, 6033–6044.

31 H. Santos Silva, H. H. Ramanitra, B. A. Bregadiolli, D. Bégué, C. F. O. Graeff, C. Dagron-Lartigau, H. Peisert, T. Chassé and

R. C. Hiorns, Oligo- and poly(fullerene)s for photovoltaic applications: Modeled electronic behaviors and synthesis, *J. Polym. Sci. Part A Polym. Chem.*, 2017, **55**, 1345–1355.

32 H. S. Silva, H. H. Ramanitra, B. A. Bregadiolli, A. Tournebize, D. Bégué, S. A. Dowland, C. Lartigau-Dagron, C. F. O. Graeff, A. Distler, H. Peisert, T. Chassé and R. C. Hiorns, In Situ Generation of Fullerene from a Poly(fullerene), *J. Polym. Sci. Part B Polym. Phys.*, 2019, **57**, 1434–1452.

33 M. Stephen, S. Dowland, A. Gregori, H. H. Ramanitra, H. Santos Silva, C. M. Combe, D. Bégué, C. Dagron-Lartigau, G. E. Morse, K. Genevičius, K. Arlauskas, G. Juška, A. Distler and R. C. Hiorns, Main-chain alternating fullerene and dye oligomers for organic photovoltaics, *Polym. Int.*, 2017, **66**, 388–398.

34 S. A. Dowland, M. Salvador, J. D. Perea, N. Gasparini, S. Langner, S. Rajoelson, H. H. Ramanitra, B. D. Lindner, A. Osvet, C. J. Brabec, R. C. Hiorns and H. J. Egelhaaf, Suppression of Thermally Induced Fullerene Aggregation in Polyfullerene-Based Multiacceptor Organic Solar Cells, *ACS Appl. Mater. Interfaces*, 2017, **9**, 10971–10982.

35 H. H. Ramanitra, S. A. Dowland, B. A. Bregadiolli, M. Salvador, H. Santos Silva, D. Bégué, C. F. O. Graeff, H. Peisert, T. Chassé, S. Rajoelson, A. Osvet, C. J. Brabec, H. J. Egelhaaf, G. E. Morse, A. Distler and R. C. Hiorns, Increased thermal stabilization of polymer photovoltaic cells with oligomeric PCBM, *J. Mater. Chem. C*, 2016, **4**, 8121–8129.

36 M. J. Frisch, G. W. Trucks, H. B. Schlegel, G. E. Scuseria, M. A. Robb, Cheeseman, J. R. G. Scalmani, V. Barone, B. Mennucci, G. A. Petersson, H. Nakatsuji, M. Caricato, X. Li, H. P. Hratchian, A. F. Izmaylov, J. Bloino, G. Zheng, J. L. Sonnenberg, M. Had and D. J. Fox., *Gaussian 09, Revis. A.02*, Gaussian, Inc., Wallingford CT, 2009.

37 C. Reichardt and T. Welton, *Solvents and Solvent Effects in Organic Chemistry*, Wiley-VCH Verlag GmbH & Co. KGaA, Weinheim, Germany, 2010.

38 D. Lacey and S. Holder, Langmuir-Blodgett films., *J. Chem. Technol. Biotechnol.*, 2007, **54**, 201–201.

39 S. Ravaine, C. Mingotaud and P. Delhaès, Langmuir and Langmuir-Blodgett films of C60 derivatives, *Thin Solid Films*, 1996, **284**–**285**, 76–79.

40 D. Felder-Flesch, Self- Or induced organization of [60]fullerene hexakisadducts, *Struct. Bond.*, 2013, **159**, 101–144.

41 W. R. Lindemann, W. Wang, F. Fungura, J. Shinar, R. Shinar and D. Vaknin, The effect of cesium carbonate on 1-(3-methoxycarbonyl)propyl-1-phenyl[6,6]C 61 aggregation in films, *Appl. Phys. Lett.*, 2014, **105**, 191605.

42 S. Lowell, J. E. Shields, M. A. Thomas and M. Thommes, 2004, pp. 58–81.

43 J. D. Swalen, Langmuir-Blodgett Films. Gareth Roberts, Ed. Plenum, New York, 1990. xiv, 425 pp., illus. $85, *Science (80-.).*, 1990, **249**, 305–306.

44 L. Liang and Y. Fang, Photoluminescence of a mixed Langmuir-Blodgett film of C60 and stearic acid at room temperature, *Spectrochim. Acta - Part A Mol. Biomol. Spectrosc.*, 2008, **69**, 113–116.

45 F. MacHui, S. Langner, X. Zhu, S. Abbott and C. J. Brabec, Determination of the P3HT:PCBM solubility parameters via a binary solvent gradient method: Impact of solubility on the photovoltaic performance, *Sol. Energy Mater. Sol. Cells*, 2012, **100**, 138–146.

46 G. E. Morse, A. Tournebize, A. Rivaton, T. Chassé, C. Taviot-Gueho, N. Blouin, O. R. Lozman and S. Tierney, The effect of polymer solubilizing side-chains on solar cell stability, *Phys. Chem. Chem. Phys.*, 2015, **17**, 11884–11897.

47 H. S. Silva, J. Cresson, A. Rivaton, D. Bégué and R. C. Hiorns, Correlating geometry of multidimensional carbon allotropes molecules and stability, *Org. Electron.*, 2015, **26**, 395–399.

48 S. G. Penn, D. A. Costa, A. L. Balch and C. B. Lebrilla, Analysis of C60 oxides and C120On (n = 1,2,3) using matrix assisted laser desorption-ionization Fourier transform mass spectrometry, *Int. J. Mass Spectrom. Ion Process.*, 1997, **169**–**170**, 371–386.

49 M. Roesing, J. Howell and D. Boucher, Solubility characteristics of poly(3-hexylthiophene), *J. Polym. Sci. Part B Polym. Phys.*, 2017, **55**, 1075–1087.

50 J. R. Baena, M. Pérez, M. Gallego, M. T. Martín-Romero, M. Valcárcel and L. Camacho, Study of a new C60 derivative at the air-water interface, *Thin Solid Films*, 2004, **449**, 215–221.

51 D. E. Motaung, G. F. Malgas and C. J. Arendse, Comparative study: The effects of solvent on the morphology, optical and structural features of regioregular poly(3-hexylthiophene):fullerene thin films, *Synth. Met.*, 2010, **160**, 876–882.

52 V. Álvarez-Venicio, M. Gutiérrez-Nava, O. Amelines-Sarria, E. Álvarez-Zauco, V. A. Basiuk and M. P. Carreón-Castro, Incorporation in Langmuir-Blodgett films of an amphiphilic derivative of fullerene C60 and oligo-para-phenylenevinylene, *Thin Solid Films*, 2012, **526**, 246–251.

53 S. Eliyahu and R. Yerushalmi-Rozen, Polymer mediated assembly of fullerenes into non-closed packed two-dimensional arrays, *Chem. Commun.*, 2010, **46**, 5966–5968.

54 A. M. Kolker and N. Y. Borovkov, Three-dimensional aggregation of fullerene C60 at the air–water interface, *Colloids Surfaces A Physicochem. Eng. Asp.*, 2012, **414**, 433–439.

55 G. Li, V. Shrotriya, Y. Yao, J. Huang and Y. Yang, Manipulating regioregular poly(3-hexylthiophene) : [6,6]-phenyl-C61-butyric acid methyl ester blends—route towards high efficiency polymer solar cells, *J. Mater. Chem.*, 2007, **17**, 3126.

56 S. Falke, P. Eravuchira, A. Materny and C. Lienau, Raman spectroscopic identification of fullerene inclusions in

polymer/fullerene blends, *J. Raman Spectrosc.*, 2011, **42**, 1897–1900.

57 J. Jin, L. S. Li, Y. Li, Y. J. Zhang, X. Chen, D. Wang, S. Jiang, T. J. Li, L. B. Gan and C. H. Huang, Structural Characterizations of C 60 -Derivative Langmuir−Blodgett Films and Their Photovoltaic Behaviors, *Langmuir*, 1999, **15**, 4565–4569.

58 C. C. H. No, D. Zhou, L. Gan, C. Luo, H. Tan and C. Huang, Langmuir - Blodgett Films and Photophysical Properties of a C 60 - Sarcosine Methyl Ester, 1996, **60**, 3150–3156.

59 J. Liu, X. Guo, Y. Qin, S. Liang, Z. X. Guo and Y. Li, Dumb-belled PCBM derivative with better photovoltaic performance, *J. Mater. Chem.*, 2012, **22**, 1758–1761.

60 S. Cook, R. Katoh and A. Furube, Ultrafast studies of charge generation in PCBM: P3HT blend films following excitation of the fullerene PCBM, *J. Phys. Chem. C*, 2009, **113**, 2547–2552.

61 A. Sassara, G. Zerza, M. Chergui, F. Negri and G. Orlandi, The visible emission and absorption spectrum of C60, *J. Chem. Phys.*, 1997, **107**, 8731–8741.

62 S. Izawa, K. Hashimoto and K. Tajima, Synthesis, characterization, and photovoltaic properties of diketopyrrolopyrrole-oligothiophene/fullerene dyads, *Synth. Met.*, 2012, **162**, 2201–2205.

63 G. W. Wang, T. H. Zhang, X. Cheng and F. Wang, Selective addition to [60]fullerene of two different radicals generated from Mn(III)-based radical reaction, *Org. Biomol. Chem.*, 2004, **2**, 1160–1163.

64 R. V. Bensasson, E. Bienvenue, M. Dellinger, S. Leach and P. Seta, C60 in model biological systems. A visible-UV absorption study of solvent-dependent parameters and solute aggregation, *J. Phys. Chem.*, 1994, **98**, 3492–3500.

65 Y.-P. Sun, B. Ma and C. E. Bunker, Effects of solvent environment on vibronic structures of the C70 fluorescence spectrum. Reverse Ham behaviour in solvent polarity dependence, *J. Chem. Soc. Chem. Commun.*, 1994, 2099.

66 K. S. Schweizer and D. Chandler, Quantum theory of solvent effects on electronic spectra: Predictions of the exact solution of the mean spherical model, *J. Chem. Phys.*, 1983, **78**, 4118–4125.

67 S. Leach, M. Vervloet, A. Desprès, E. Bréheret, J. P. Hare, T. John Dennis, H. W. Kroto, R. Taylor and D. R. M. Walton, Electronic spectra and transitions of the fullerene C60, *Chem. Phys.*, 1992, **160**, 451–466.

68 C. A. Sandstedt, R. D. Rieke and C. J. Eckhardt, Solid-State and Solvatochromic Spectra of a Highly Regular Polythiophene, *Chem. Mater.*, 1995, **7**, 1057–1059.

69 G. Dicker, T. J. Savenije, B.-H. Huisman, D. M. de Leeuw, M. P. de Haas and J. M. Warman, Photoconductivity enhancement of poly(3-hexylthiophene) by increasing inter- and intra-chain order, *Synth. Met.*, 2003, **137**, 863–864.

70 T. A. Chen, X. Wu and R. D. Rieke, Regiocontrolled Synthesis of Poly(3-alkylthiophenes) Mediated by Rieke Zinc: Their Characterization and Solid-State Properties, *J. Am. Chem. Soc.*, 1995, **117**, 233–244.

71 D. E. Motaung, G. F. Malgas, C. J. Arendse, S. E. Mavundla and D. Knoesen, Structural and photo-physical properties of spin-coated poly (3-hexylthiophene) thin films, 2009, **116**, 279–283.

72 A. L. Ayzner, C. J. Tassone, S. H. Tolbert and B. J. Schwartz, Reappraising the Need for Bulk Heterojunctions in Polymer - Fullerene Photovoltaics : The Role of Carrier Transport in All-Solution-Processed P3HT / PCBM Bilayer Solar Cells, 2009, 20050–20060.

73 L. K. M. Roncaselli, E. A. Silva, H. H. Ramanitra, M. Stephen, A. V. S. Simõis, D. Bégué, D. L. S. Agostini, R. C. Hiorns and C. A. Olivati, Study of the Effect of Solvent on the Conductivity of Langmuir-Schaefer Films of Poly(Fullerene)s, *Mater. Res.*, , DOI:10.1590/1980-5373-mr-2021-0028.

74 C. Poelking, K. Daoulas, A. Troisi and D. Andrienko, 2014, pp. 139–180.

75 T. Kambayashi, M. Goto, M. Ofuji, T. Mori, H. Takezoe and K. Ishikawa, Doping Effect on Surface Roughness of Organic Semiconductor Thin Films, *Jpn. J. Appl. Phys.*, 2006, **45**, 526–529.

76 X. Wang, D. Zhang, K. Braun, H. J. Egelhaaf, C. J. Brabec and A. J. Meixner, High-Resolution spectroScopic mapping of the chemical contrast from nanometer domains in P3HT:PCBM organic blend films for Solar-Cell applications by, *Adv. Funct. Mater.*, 2010, **20**, 492–499.

77 X. Wang, H. J. Egelhaaf, H. G. Mack, H. Azimi, C. J. Brabec, A. J. Meixner and D. Zhang, Morphology related photodegradation of low-band-gap polymer blends, *Adv. Energy Mater.*, 2014, **4**, 1–12.

78 E. A. Silva, A. Gregori, J. D. Fernandes, C. Njel, R. Dedryvère, C. J. L. Constantino, R. C. Hiorns, C. Lartigau-Dagron and C. A. Olivati, Understanding the langmuir and Langmuir-Schaefer film conformation of low-bandgap polymers and their bulk heterojunctions with PCBM, *Nanotechnology*, 2020, **31**, 315712.

79 D. C. Bento, E. A. da Silva, C. de Almeida Olivati, G. Louarn and H. de Santana, Characterization of the interaction between P3ATs with PCBM on ITO using in situ Raman spectroscopy and electrochemical impedance spectroscopy, *J. Mater. Sci. Mater. Electron.*, 2015, **26**, 7844–7852.

80 H. Kuzmany, R. Pfeiffer, M. Hulman and C. Kramberger, *Philos. Trans. R. Soc. A Math. Phys. Eng. Sci.*, 2004, 362, 2375–2406.

81 D. E. Motaung, G. F. Malgas and C. J. Arendse, Comparative study: The effects of solvent on the morphology, optical and structural features of regioregular poly(3-hexylthiophene):fullerene thin films, *Synth. Met.*, 2010,

160, 876–882.

82 K. Lewandowska, B. Barszcz, A. Graja, S. Y. Nam, Y. S. Han, T. D. Kim and K. S. Lee, Spectroscopic properties and orientation of molecules in Langmuir-Blodgett layers of selected functionalized fullerenes, *Spectrochim. Acta - Part A Mol. Biomol. Spectrosc.*, 2014, **118**, 204–209.